ELSEVIER

Chemical Engineering Journal 81 (2001) 223–230

Chemical Engineering Journal

www.elsevier.com/locate/cej

A highly elevated mass transfer rate process for three-phase, liquid-continuous fluidized beds

Chia-Min Chen, Lii-Ping Leu*

Department of Chemical Engineering, National Taiwan University, Taipei 106-17, Taiwan

Received 13 March 1999; received in revised form 9 February 2000; accepted 11 February 2000

Abstract

Average gas holdup and gas-to-liquid mass transfer in three-phase fluidized beds with non-Newtonian fluids were studied. The effects of liquid property, gas distributor type and magnetic field intensity on mass transfer coefficient and overall gas holdup were examined. The volumetric gas-to-liquid mass transfer coefficient was determined by fitting the oxygen concentration profile data across the bed to the axial dispersion model. The average gas holdup and mass transfer coefficient were all correlated with operating parameters including gas velocity and effective viscosity.

Experimental results showed that a three-fold increase in mass transfer coefficient and a two-fold increase in average gas holdup were observed with properly designed liquid property and gas distributor. A modified process was developed to highly elevate the volumetric gas-to-liquid mass transfer rate. The bubble coalescing property of three-phase fluidized beds with small particles is eliminated, and its application to biotechnology and enzyme-catalyzed processes with high gas-to-liquid mass transfer rate could be achieved.

Keywords: Three-phase fluidized beds; Mass transfer; Gas holdup; Non-Newtonian fluid

1. Introduction

Typical applications of three-phase fluidized beds are enzyme-catalyzed reactions, polymerization reactions and biotechnology processes. In his review on gas–liquid–solid fluidization in biotechnology, Schugerl [1] listed aerobic and anaerobic waste-water treatment, cultivation of immobilized and pellet-forming microorganisms, animal and plant cells. Several attempts have been made to develop bioreactors by taking advantage of the features of three-phase fluidized beds such as high contacting efficiency between different phases, high heat and mass transfer rates and low pressure drop.

Operating conditions applied in biotechnology processes employed carrier-particle diameters ranging from 0.2 to 0.5 mm; superficial liquid velocity ranging from 0.01 to 0.05 m/s. Low liquid and gas velocities were employed to match the slow biological reaction rates and to prevent excessive sloughing of biofilms or particle–particle attrition. Only few engineering data concerning gas-to-liquid mass transfer were published on three-phase fluidized beds containing small particles with mean diameter smaller than 1 mm [2]. While bubble coalescence commonly occurs and was attributed to the liquid–solid suspension acting as a pseudo-homogeneous medium of higher apparent viscosity than those of the liquid medium alone. The mass transfer rate in three-phase fluidized beds with relatively small particles are lower than those with large particles due to the bubble coalescence. So the application of such system is limited because of the low mass transfer rate compared to the larger particles.

The relationship between packed volume of solid phase and particle diameter can be expressed as follows:

$$(1 - \varepsilon_l - \varepsilon_g)V = N\left(\frac{\pi}{6}D_p^3\right) \tag{1}$$

and the exposed area of solid phase can be written as

$$N(\pi D_p^2) = \frac{6(1 - \varepsilon_l - \varepsilon_g)V}{D_p} \tag{2}$$

It can be seen from Eq. (2) that the exposed area of solid phase per unit volume is inversely proportional to the particle diameter. It means the contact area between solid and liquid–gas phase is higher in three-phase fluidized beds containing small particles than large ones. Once the bubble coalescing property is eliminated, the contact efficiency would be higher for three-phase fluidized beds containing small particles.

* Corresponding author. Tel.: +886-2-363-5230; fax: +886-2-362-3040.

1385-8947/01/$ – see front matter
PII: S1385-8947(00)00196-0

Nomenclature

a	parameter in Eq. (8)
b	parameter in Eq. (8)
C	concentration of oxygen (mg/dm^3)
C_0	inlet concentration of oxygen (mg/dm^3)
C^*	equilibrium dissolved oxygen concentration (mg/dm^3)
D_a	axial dispersion coefficient (m^2/s)
D_p	particle diameter (m)
H	applied magnetic field intensity (A/m)
I	increment of average gas holdup
k	fluid consistency index (Pa s^n)
k_{La}	gas-to-liquid mass transfer coefficient (1/s)
k_{La,H_2O}	gas-to-liquid mass transfer coefficient in air–water–nickel system (1/s)
L	axial distance (m)
N	number of particles
n	flow behavior index
Pe	axial Peclet number
St	Stanton number
U_l	superficial liquid velocity (m/s)
U_g	superficial gas velocity (m/s)
V	packed volume of particles (m^3)
Z	dimensionless axial position

Greek letters

ε_g	average gas fraction
ε_{g,H_2O}	average gas fraction in air–water–nickel system
$\varepsilon_{g,H=0}$	average gas fraction without magnetic field
ε_l	liquid fraction
μ_{H_2O}	viscosity of water (Pa s)
μ_{eff}	effective viscosity (Pa s)
γ	shear rate (1/s)

The enhancement of mass transfer rate with bubble breakage by large particles has been applied to three-phase fluidized bed operation. Kim and Kim [3] and Kang et al. [4] employed floating bubble breakers made of a mixture of lead particles and paraffin fluidized in an air–water bed containing glass beads with sizes varying from 1 to 6 mm. They found that the volumetric mass transfer coefficient is enhanced as much as 25% by adding the floating bubble breakers to the bed, and the mass transfer coefficient exhibits a maximum value with respect to the volume ratio of floating breakers to the fluidized particles. Kim and Kang [5] examined the heat and mass transfer characteristics in three-phase fluidized beds, and various correlations and models to predict the heat and mass transfer coefficients in the literature have been examined.

The type of gas distributor was observed to have a considerable influence on gas holdup during an investigation of three-phase fluidized beds. So, in this study the effect of liquid property, type of gas distributor and magnetic field intensity on mass transfer coefficient and overall gas holdup of three-phase fluidized beds were examined.

2. Experimental

Fig. 1 shows a schematic diagram of the experimental apparatus. Water flows through a 0.05 m i.d., 0.5 m long plexiglas column loaded with spherical shaped nickel powders of average diameter 0.194 mm (ranging from 0.177 to 0.21 mm). The density of the nickel powders is 8900 kg/m^3. Sampling ports are placed at 0.1 m intervals along the column. A perforated plate with 48 evenly spaced holes of 1.0 mm diameter and fractional free area 2.0% was designed to prevent liquid channeling and used as a liquid distributor for the bed. The superficial liquid velocity was set at 0.02 m/s. A Helmholtz electromagnet comprising of two coils having an inner diameter of 0.16 m and separated by a gap of 0.08 m produces an uniform and time-invariant magnetic field intensity up to a maximum value of 23,880 A/m. Power for the solenoid was provided by a DC power supply (Takasago, EX-375L) rated at 4.8 A and 27 V. A holding tank containing water is continually sparged with nitrogen gas until the dissolved oxygen concentration is negligible to the air-saturation value.

The properties of liquids used in this work are listed in Table 1, the rheological behavior of the solutions was investigated with a concentric cylinder viscometer. The concentration of the carboxymethyl cellulose (CMC) solutions varied from 0.1 to 1.5 wt.%, and their rheological properties can be described by the power-law model. The relationship between the effective viscosity and shear rate of non-Newtonian fluid can be written as follows:

$$\mu_{eff} = k\gamma^{n-1} \tag{3}$$

where k and n are the fluid consistency index and flow behavior index, respectively. The CMC solution exhibiting pseudo-plastic flow behavior and the effective shear rate can be written as follows (Schumpe et al. [6]):

$$\gamma = 2800\left(U_g - U_l\frac{\varepsilon_g}{\varepsilon_l}\right) \tag{4}$$

Table 1
Physical properties and flow parameters of viscous liquid media[a]

Liquid	n	k (Pa s^n)	ρ (kg/m^3)
Water	1	0.001	1001
0.1 wt.% CMC	0.975	0.0022	1001
0.25 wt.% CMC	0.943	0.0028	1002
0.5 wt.% CMC	0.893	0.0061	1003
0.75 wt.% CMC	0.842	0.0098	1005
1.0 wt.% CMC	0.801	0.028	1005
1.5 wt.% CMC	0.765	0.081	1006

[a] $\mu_{eff} = k\gamma^{n-1}$.

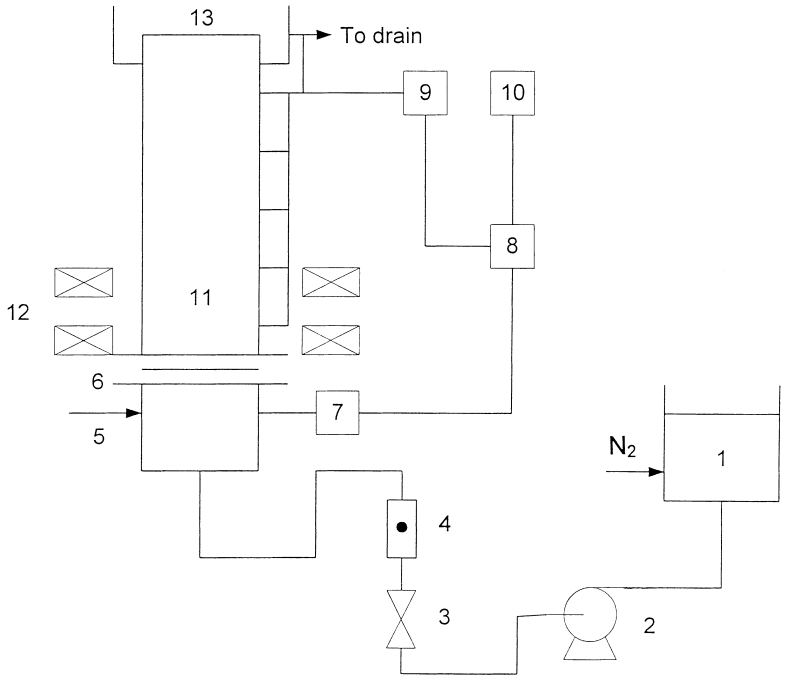

1. stripping tank
2. centrifugal pump
3. globe valve
4. rotameter
5. gas inlet
6. distributor
7. pressure transducer
8. data acquisition system
9. DO meter
10. personal computer
11. fluidized bed
12. Helmholtz coils
13. screen

Fig. 1. Experimental setup.

The effective viscosity of CMC solutions has been determined from Eqs. (3) and (4). Three different types of gas distributor used are listed in Table 2. Thirty-six holes were drilled evenly spacing through the ring sparger. Type I gas distributor has been widely used (Nguyen-tien et al. [2], Kang et al. [4], Schumpe et al. [6], Patwari et al. [7], Lee et al. [8]), and they found that the gas-to-liquid mass transfer coefficient decreases exponentially with increasing effective viscosity.

The valve technique [9] was used to measure the average gas holdup over the entire bed. This was accomplished by shutting off the gas and liquid flows and measuring the static liquid height. The average gas holdup was calculated by dividing the trapped gas volume by the total bed volume. The steady state method [10] was used to calculate the gas-to-liquid mass transfer coefficient k_{La}. A mass balance on oxygen in the liquid phase of the bed is shown as

$$\frac{1}{Pe}\frac{d^2C}{dZ^2} - \frac{dC}{dZ} - St\,C = -St\,C^* \tag{5}$$

where the Peclect number, *Pe*, and Stanton number, *St*, are defined as

$$Pe = \frac{U_l L}{D_a \varepsilon_l} \tag{6}$$

$$St = \frac{k_{La} L}{U_l} \tag{7}$$

The equilibrium dissolved oxygen concentration C^* is the function of the depth of bed, thus

$$C^* = a + bZ \tag{8}$$

And the following boundary conditions are required:

$$Z = 0, \qquad C = C_0 + \frac{1}{Pe}\frac{dC}{dZ} \tag{9}$$

$$Z = 1, \qquad \frac{dC}{dZ} = 0 \tag{10}$$

Table 2
Gas distributor design

Type	Hole diameter (m)	Number of holes
I	0.001	36
II	0.0005	36
III	0.0001	36

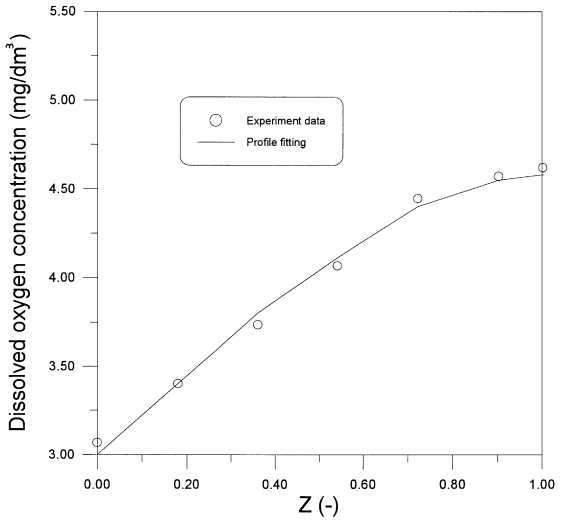

Fig. 2. Comparison between profile fitting and axial dissolved oxygen profile.

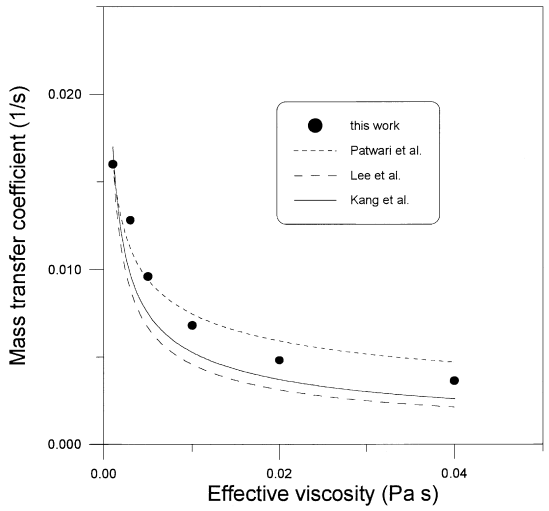

Fig. 3. Effect of effective viscosity on mass transfer coefficient in three-phase fluidized beds (gas velocity=0.02 m/s).

The gas-to-liquid mass transfer coefficient and axial dispersion coefficient were obtained by parameter fitting of analytical solution of Eqs. (5)–(10) to the experimental dissolved oxygen concentration profile across the bed. A non-linear statistical regression program was employed for the parameter fitting, which gives a minimum value of the sum of squares of the error. One typical example of profile fitting is shown in Fig. 2.

3. Results and discussion

3.1. Liquid side mass transfer resistance

The effect of non-Newtonian fluid behavior on mass transfer coefficient has been studied by several investigators (Kim and Kim [3], Kang et al. [4], Kim and Kang [5], Schumpe et al. [6], Patwari et al. [7], Lee et al. [8]), and they found that the mass transfer coefficient decreased with increasing effective viscosity. Schumpe et al. [6] and Patwari et al. [7] found that the mass transfer coefficient depends upon the effective viscosity to a power of −0.34, while Lee et al. [8] found that this value was −0.548 to −0.671. Kang et al. [4] found that this value was −0.52 in three-phase fluidized beds with floating bubble breakers. Fig. 3 shows the result obtained from this work with distributor type I, it is similar to those described above. The mass transfer coefficient depends upon the effective viscosity to a power of −0.42, the correlation of Patwari et al. [7] and Schumpe et al. [6] are slightly higher than those of the present study, and the correlations of Lee et al. [8] and Kang et al. [4] are lower than those of this study. The difference may be due to the different particle size and rheological properties.

It was explained that the decrease of mass transfer coefficient with increasing effective viscosity is attributed to the increase of local liquid holdup, which leads to the increase of bubble diameter and the decrease of contact frequency and area between the gas bubbles and liquid media. The behavior of rising bubbles became restricted with the increase of effective viscosity due to the enhancement in the drag force acting on the gas bubbles, which leads to serious bubble coalescence and increase the bubble diameter. Miyahara et al. [11] reported that the Sauter mean bubble diameter depends upon the effective viscosity to a power of 0.168 in external-loop airlift bubble column, which leads to a decrease of interfacial area with increasing effective viscosity. The effect of non-Newtonian fluid behavior on gas bubbles showed similar trend in both bubble column and three-phase fluidized beds.

3.2. Effect of gas distributor design on k_{La} and gas holdup

The flow regime in three-phase fluidized beds classified by the gas bubble behavior have been reported by Kim et al. [9], there are three flow regimes including coalesced bubble, dispersed bubble (bubble disintegrating) and slug flow. The flow regime map of three-phase fluidized beds classified by the gas bubble behavior is shown in Fig. 4. In the coalesced bubble regime, bubbles tend to coalesce and the shape of bubble is spherical-cap. While in the dispersed bubble regime, no bubble coalescence occurs and the bubbles are of spherical shape with small size. The boundary between dispersed bubble and coalesced bubble is independent of gas velocity, the regime of dispersed bubble was expanded with proper designed gas distributor and liquid property.

Page and Harrison [12] reported that the bubble size depends strongly on the type of gas distributor. Miyahara et al. [11] found that the Sauter mean bubble diameter decreased with decreasing hole diameter in external-loop airlift bubble column. The effect of gas velocity and type of gas distributor on mass transfer coefficient is shown in Fig. 5.

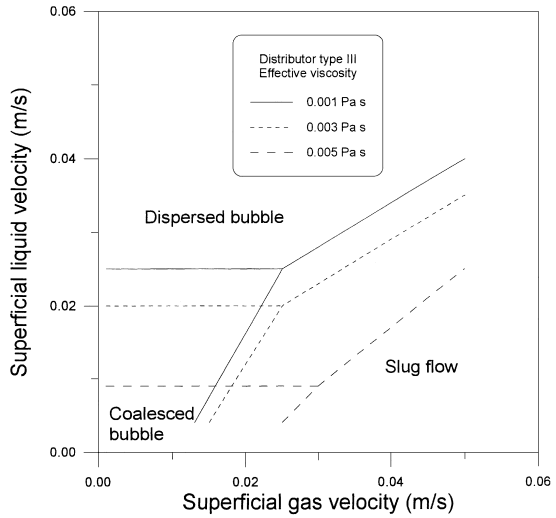

Fig. 4. The flow regime map of three-phase fluidized beds with non-Newtonian fluids.

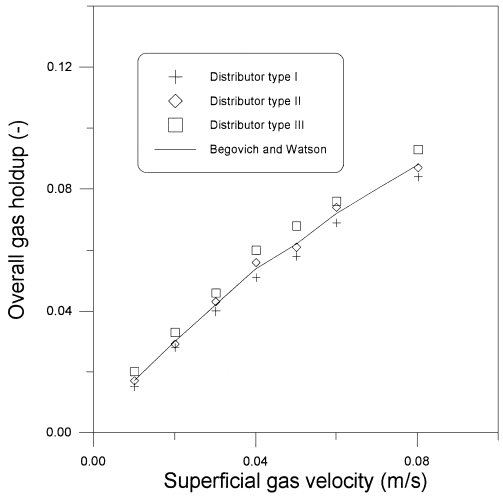

Fig. 6. Effect of gas distributor type and gas velocity on overall gas holdup.

The mass transfer coefficient increased with increasing gas velocity and with decreasing hole diameter. The bubble size was observed to decrease with decreasing hole diameter and enhanced the gas–liquid contact area. The correlation of mass transfer coefficient obtained from Nguyen-tien et al. [2] gave values 16% higher than those measured with type I gas distributor, and 10% lower than those with type III gas distributor. A 26% difference of mass transfer coefficient was observed in air–water–nickel system with different gas distributor type. The correlation of mass transfer coefficients obtained from Kim and Kim [3] and Kang et al. [4] gave reasonable agreement with this work.

Fig. 6 shows the effect of gas velocity and type of gas distributor on average gas holdup. The average gas holdup increases with increasing gas velocity, and the effect of hole diameter of gas distributor on average gas holdup is not significant and can be neglected. The average gas fraction data are compared to a correlation published by Begovich and Watson [13] in Fig. 6. Despite the differences in particle density and rheological properties the data here are in good agreement with their correlation.

3.3. Optimum design of gas distributor and liquid property

The effect of effective viscosity and gas distributor type on mass transfer coefficient is shown in Fig. 7, where mass transfer coefficient decreased exponentially with effective viscosity with type I and type II gas distributor since liquid diffusivity decreased with increasing effective viscosity. Also, the interfacial area decreased with an increase in

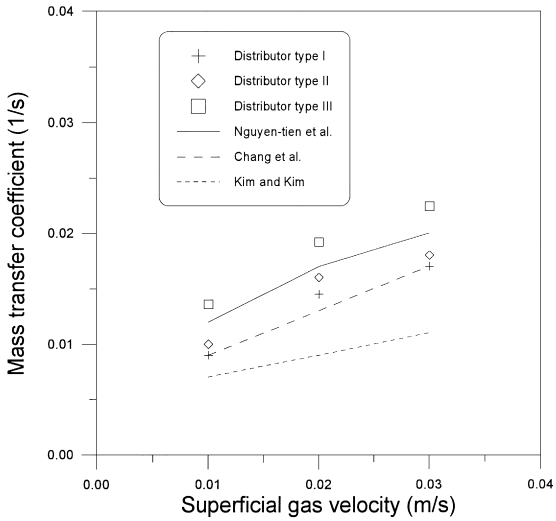

Fig. 5. Effect of gas distributor type and gas velocity on mass transfer coefficient.

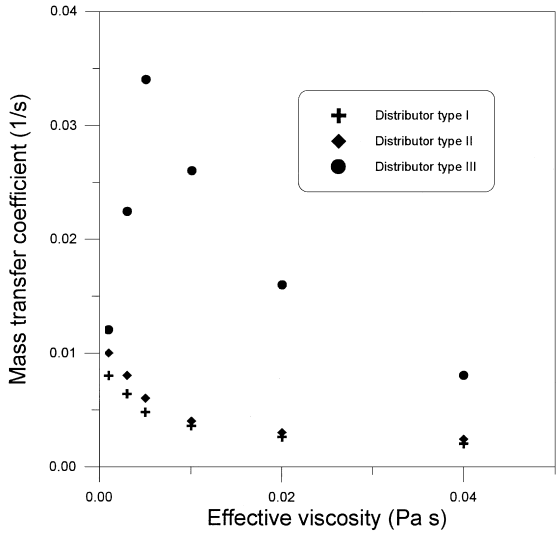

Fig. 7. Effect of distributor type and effective viscosity on mass transfer coefficient (gas velocity=0.01 m/s).

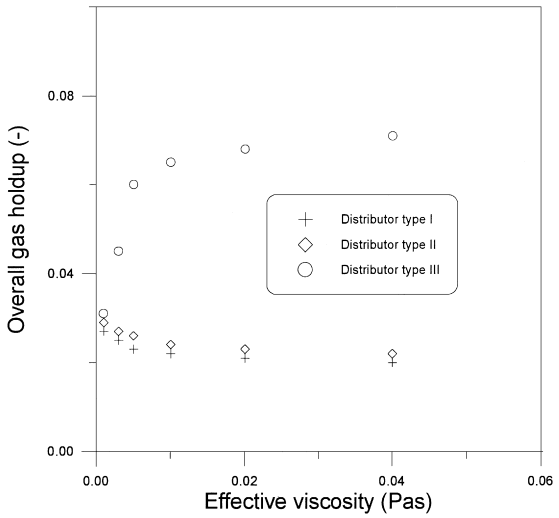

Fig. 8. Effect of distributor type and effective viscosity on overall gas holdup (gas velocity=0.02 m/s).

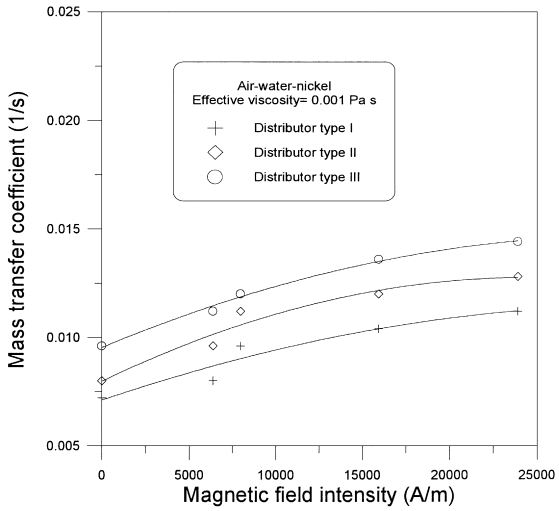

Fig. 9. Mass transfer coefficient as a function of magnetic field intensity (gas velocity=0.01 m/s).

effective viscosity since bubble size increased with effective viscosity.

A converse result was observed where the mass transfer coefficient increases with increasing effective viscosity from low to medium concentration of CMC solution with type III gas distributor, the bubble coalescing property was eliminated and the bubble size was observed smaller than those in air–water–nickel system. A three-fold increase in mass transfer coefficient was observed in medium concentration of CMC solution, while the average gas holdup shown in Fig. 8 indicated a two-fold increase in average gas holdup at the same condition. The gas bubble was observed non-coalescing and remained the same size across the whole bed. And the mass transfer coefficient decreased with increasing effective viscosity from medium to high concentration. The average gas holdup with gas distributor type I and type II can be correlated by the following equation (all units in SI):

$$\varepsilon_g = 0.143 U_g^{0.82} \mu_{eff}^{-0.08} \tag{11}$$

Two competition factors involved are: (i) increased liquid side resistance due to the non-Newtonian fluid behavior, (ii) increased average gas holdup due to the non-coalescing property of liquid. The first one dominated the effect of decreasing mass transfer coefficient from medium to high effective viscosity, while the second one dominated the effect of increasing mass transfer coefficient from low to medium effective viscosity. Bubble size was observed to decrease with increasing effective viscosity from low to medium effective viscosity, so the increased gas holdup highly effected the mass transfer rate. And the bubble size decreases slightly from medium to highly effective viscosity, the increased liquid side resistance dominated the effect rather than the bubble property.

The liquid side resistance depends upon the effective viscosity to a power of 0.42, the combination of effect of liquid side resistance and gas holdup on mass transfer coefficient could be written as follows (all units in SI):

$$\frac{k_{La}}{k_{La,H_2O}} = \left(\frac{\mu_{eff}}{\mu_{H_2O}}\right)^{-0.42} \left(\frac{\varepsilon_g}{\varepsilon_{g,H_2O}}\right)^{2.1} \tag{12}$$

3.4. Effect of magnetic field on k_{La} and gas holdup

The effect of magnetic field on mass transfer coefficient of three-phase fluidized beds has been known to reduce the mass transfer resistance [14]. Figs. 9–11 show the effect of magnetic field intensity on mass transfer coefficient in air–water–nickel and air–CMC–nickel systems. The mass transfer coefficient increases with increasing magnetic field intensity in all cases, while the effect of enhancement in air–water–nickel system was nearly proportional to mag-

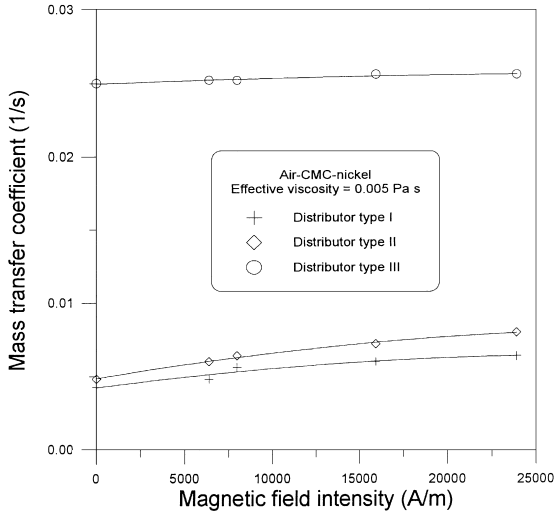

Fig. 10. Mass transfer coefficient as a function of magnetic field intensity (gas velocity=0.01 m/s).

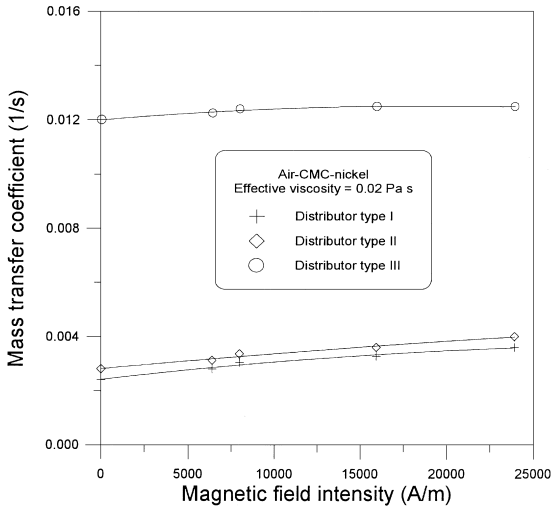

Fig. 11. Mass transfer coefficient as a function of magnetic field intensity (gas velocity=0.01 m/s).

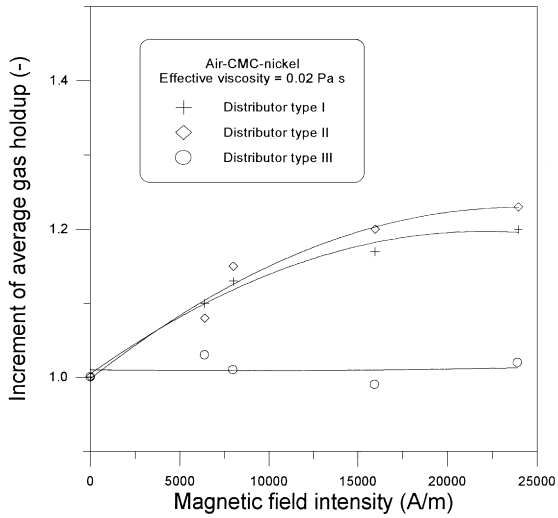

Fig. 13. Increment of average gas holdup as a function of magnetic field intensity (gas velocity=0.02 m/s).

netic field intensity. The highest increase of mass transfer coefficient was about 50%.

Ouyang et al. [15] and Kwauk et al. [16] reported that the bubble diameter decreases with increasing magnetic field intensity. A similar result was observed in this work, the addition of magnetic field resulted in bed contraction and smaller bubbles. In this study, the average gas holdup increases with increasing magnetic field intensity. With the decreasing of bubble size, the gas–liquid interfacial area was increased and the mass transfer coefficient was increased.

The magnetic field had almost no effect on mass transfer coefficient in air–CMC–nickel system with distributor type III, it is due to the bubble coalescing property that was eliminated from that described above even with no magnetic field. The increment of average gas holdup is defined as follows:

$$I = \frac{\varepsilon_g}{\varepsilon_{g,H=0}} \tag{13}$$

Figs. 12 and 13 show the effect of magnetic field intensity on increment of average gas holdup in air–CMC–nickel system. The variations of increment are raised from 1.0 without magnetic field to about 1.2 with high magnetic field intensity with type I and II distributor. And the magnetic field had almost no effect on increment with type III distributor, it means the bubble property did not change with the addition of magnetic field.

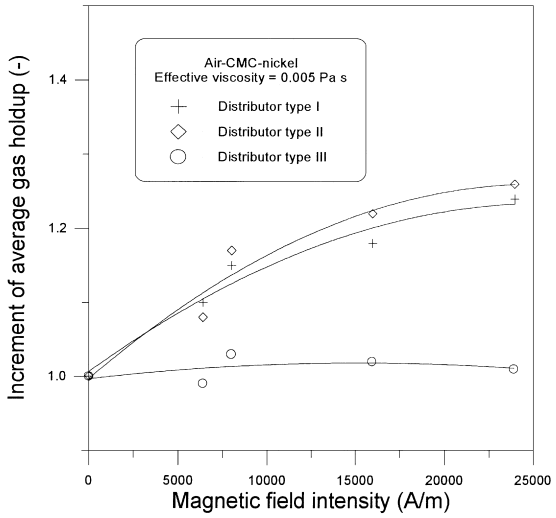

Fig. 12. Increment of average gas holdup as a function of magnetic field intensity (gas velocity=0.02 m/s).

4. Conclusions

The effect of non-Newtonian flow behavior and gas distributor type on mass transfer coefficient and average gas holdup were studied. The mass transfer coefficient and gas holdup increased with decreasing effective viscosity and decreasing distributor hole diameter with type I and II gas distributor, a three-fold increase in mass transfer coefficient and two-fold increase in average gas holdup was observed with gas distributor type III in medium concentration of CMC solution. The magnetic field have positive effect on gas-to-liquid mass transfer coefficient and average gas holdup in three-phase fluidized beds with non-Newtonian fluids.

With proper designed liquid property and gas distributor, the bubble coalescing property was eliminated and highly elevate the mass transfer coefficient. The application of three-phase fluidized beds containing small particles with high mass transfer rate to biotechnology and enzyme-catalyzed processes could be achieved. More systematic experimental work is needed for further understanding of bubble behaviors including coalescence and breakup

natures in three-phase fluidized beds with non-Newtonian fluids and different gas distributor types.

Acknowledgements

The authors are grateful to the National Science Council, ROC, for financial support.

References

[1] K. Schugerl, Three-phase-biofluidization — application of three-phase-fluidization in the biotechnology — a review, Chem. Eng. Sci. 52 (1997) 3661–3668.
[2] K. Nguyen-Tien, A.N. Patwari, A. Schumpe, W.D. Deckwer, Gas–liquid mass transfer in fluidized particle beds, AIChE J. 31 (1985) 194–201.
[3] J.O. Kim, S.D. Kim, Gas–liquid mass transfer in a three-phase fluidized bed with floating bubble breakers, Can. J. Chem. Eng. 68 (1990) 368–375.
[4] Y. Kang, L.T. Fan, B.T. Min, S.D. Kim, Promotion of oxygen transfer in three-phase fluidized-bed bioreactors by floating bubble breakers, Biotechnol. Bioeng. 7 (1991) 580–586.
[5] S.D. Kim, Y. Kang, Heat and mass transfer in three-phase fluidized-bed reactors — a review, Chem. Eng. Sci. 52 (1997) 3639–3660.
[6] A. Schumpe, W.D. Deckwer, K.D.P. Nigam, Gas–liquid mass transfer in three-phase fluidized beds with viscous pseudoplastic liquids, Can. J. Chem. Eng. 67 (1989) 873–877.
[7] A.N. Patwari, K. Nguyen-Tien, A. Schumpe, W.D. Deckwer, Three-phase fluidized beds with viscous liquid: hydrodynamics and mass transfer, Chem. Eng. Commun. 40 (1986) 49–65.
[8] D.H. Lee, J.O. Kim, S.D. Kim, Mass transfer and phase holdup characteristics in three-phase fluidized beds, Chem. Eng. Commun. 119 (1993) 179–196.
[9] S.D. Kim, C.G. Baker, M.A. Bergougnou, Holdup and axial mixing characteristics of two and three phase fluidized beds, Can. J. Chem. Eng. 50 (1972) 695–701.
[10] W.D. Deckwer, K. Nguyen-Tien, A. Schumpe, Y. Serpemen, Oxygen mass transfer into aerated CMC solutions in a bubble column, Biotechnol. Bioeng. 24 (1982) 461–481.
[11] T. Miyahara, H. Hamanaka, T. Umeda, Y. Akagi, Effect of plate geometry on characteristics of fluid flow and mass transfer in external-loop airlift bubble column, J. Chem. Eng. Japan 32 (1999) 689–695.
[12] R.E. Page, D. Harrison, The size distribution of gas bubbles leaving a three-phase fluidized bed, Powder Technol. 6 (1972) 245–249.
[13] J.M. Begovich, J.S. Watson, Hydrodynamic characteristics of three-phase fluidized beds, in: J.F. Davidson, L. Kearins (Eds.), Fluidization, Cambridge University Press, Cambridge, UK, 1978, pp. 190–195.
[14] C.-M. Chen, L.-P. Leu, Hydrodynamics and mass transfer in three-phase magnetic fluidized beds, Powder Technol., 1999, submitted for publication.
[15] F. Ouyang, Y. Wu, C. Guo, M. Kwauk, Fluidization under external forces (I) magnetized fluidization, J. Chem. Ind. Eng. (China) 5 (1990) 206–222.
[16] M. Kwauk, X. Ma, F. Ouyang, Y. Wu, D. Weng, L. Chang, Magneto-fluidized G/L/S systems, Chem. Eng. Sci. 47 (1992) 3467–3474.